Priprem et al., 1:4
http://dx.doi.org/10.4172/scientificreports.232

Open Access Scientific Reports

Research Article Open Access

Intranasal Delivery of Nanosized Melatonin-Encapsulated Niosomes in Rats

Aroonsri Priprem[1],*, Wanwisa Limphirat[2], Sucharat Limsitthichaikoon[1], Jeffrey R. Johns[1], Pramote Mahakunakorn[1]

[1] *Faculty of Pharmaceutical Science, Khon Kaen University, 123 Mitraparb Road, Muang District, Khon Kaen, 40002 Thailand*
[2] *Synchrotron Light Research Institute, 111 University Avenue, Muang District, Nakhon Ratchasima, 30000 Thailand*

Abstract

Encapsulation of melatonin by niosomes for intranasal delivery was developed to serve the purpose as a supportive care adjuvant in cancer patients with certain conditions such as unconsciousness or GI disturbance due to side effects of chemotherapy, and to avoid its high first pass metabolism. Intranasal administration of melatonin niosomes to male Wistar rats (average body weight 150 g) at a daily dose of 20 mg/kg/d for 90 days did not show histological changes when compared to its control. FTIR of the nasal epithelium, liver, hypothalamus and testis detected some possible effect of melatonin on the membranous lipids and proteins. Melatonin niosomes of about 100 nm, intranasally administered, could distribute melatonin to the liver, hypothalamus and testis.

Keywords: Melatonin; Niosomes; Nasal delivery; Liver hypothalamus; Testis

Introduction

A nanosized formulation is a promising candidate in novel drug delivery by encapsulating, entrapping or solubilizing the drug substance which is then readily able to penetrate physiological barriers until reaching the target site(s), such as deep as the nucleus [1-4]. Thus novel developments in drug encapsulation wan overcome barriers to existing treatments [5]. Niosomes, as potential nanosized vesicles [6-8], can encapsulate various active compounds and promote cellular uptake [8-11], improve chemical stability [9-11] and reduce side effects [12]. Utilizing synthetic surfactants as bilayer components improves the chemical stability of niosomes compared to lipsomes, that are composed of natural lipids [10].

Melatonin, an endogenous neuroendocrine hormone, known as a sleep inducer, particularly in jet lag, acts as an adjuvant in cancer chemotherapy since it reduces adverse events, improves quality of life and sleep, increases survival and reduces cancer recurrence [13-16]. Intranasal melatonin was shown to be bioequivalent to intravenous injection [17] and thus which provides an option for supportive care in chemotherapy particularly with unconscious patients and/or those with GI side effects [18-20]. Also, nasal instillation could systemically deliver more controlled doses of melatonin by bypassing its extensive and highly variable first pass metabolism [19,20]. The major concern of intranasal dosage is the limited volume of instillation of about 0.4 ml or 0.2 ml per nostril [24] in human and a total of about 0.05 ml in rats [19,20], thus a nanocarrier should be a powerful tool in reducing the dose and transport the drug to inner organs. There are significant challenges in preparing concentrated melatonin in a readily absorbable form for intranasal dosing. The actual dose of melatonin is another issue, as various levels are reported for humans e.g. oral doses at 2-5 mg as a sleeping aid due to jet lag and sleep disorders, 10-20 mg for thermal injury and 20-40 mg/d in cancer [25]. Investigations on tissue distribution by solvent extraction method after exogeneous melatonin indicate that the liver, brain, testis and GI tract can cumulate melatonin [21]. Subcellular distribution of melatonin was found to be highest in the cell membrane, followed by mitochondria, nucleus and cytosol, respectively [22].

Fourier Transform Infrared (FTIR) spectroscopy has been immensely improved to provide an acceptable tool for detection of cellular and subcellular compontents, such as tissue damage [23,26,29,30]. Solvents for extraction and isolation of samples are not needed, reducing the problems with effects on confirmations and structure of complex biomolecules such as proteins, lipids and carbohydrates [31]. Thus, intact normal and diseased tissue samples, including malignancies, can be differentiated by identifying the chemical compositions of macromolecules of the complex biological samples under observation [26]. Spectral groups or clusters of selected bands can be identified and correlated by multivariate analysis [27]. Since melatonin was found to disorient membrane lipids [22,28], utilizing FTIR in analysis of tissues without solvent extraction could be a rapid and novel approach in this aspect. Partial Least Squares Discriminant Analysis (PLS-DA) [33], a powerful chemometric method to reveal variances or combination of variables among multivariate data, was applied to infrared spectra for handling the large data sets without preliminary assumption.

Nasal delivery deals with substantially small volumes of instillation which might draw criticism as to whether the instilled doses could distribute encapsulated drug to inner organs. Thus, in this study FTIR was used to observe and detect changes in selected organs after nasal delivery of nanosized-melatonin niosomes to rats.

Materials and Methods

Melatonin was purchased from Huanggang Innovation Biochemicals (China). Cholesterol (chol), sorbitan monostearate 60 (span60), dimethyl sulfoxide and sodium deoxycholate (SDC) were from Sigma (U.S.A.). Chloroform and ethanol were purchased from BDH Laboratory Supplies (England). Glycerin was from Vidhyasom (Thailand). Pentobarbital sodium (54.7 mg/ml) was from CEVA Santé Animale (France). All were used as technical grade.

***Corresponding author:** Aroonsri Priprem, Faculty of Pharmaceutical Science, Khon Kaen University, 123 Mitraparb Road, Muang District, Khon Kaen, 40002 Thailand, Tel: +66-43-202378 ext 1403; Fax: +66-43-362092; Email: aroonsri@kku.ac.th

Received March 16, 2012; **Published** August 06, 2012

Citation: Priprem A, Limphirat W, Limsitthichaikoon S, Johns JR, Mahakunakorn P (2012) Intranasal Delivery of Nanosized Melatonin-Encapsulated Niosomes in Rats. 1: 232. doi:10.4172/scientificreports.232

Deionized water (water) and some reagents were purified by the Milli-Q system (Sartorius GMBH Gottingen, Germany). The extruder (Lipex, Canada), polycarbonate membrane was from Whatman (U.S.A.). Ultracentrifuge was from Sorvall (U.S.A.) and Pharmaspec UV-visible spectrophotometer from Shimadzu (Japan). Humidified CO_2 incubator (Shell Lab, U.S.A.), Axiovert 25 inverted microscope (Carl Zeiss Microscopy, U.S.A.), centrifuge (Kubota 6200, Japan), Olympus microscopy (AxioCam, Germany), microplate reader (Bio Rad, Japan), ultramicrotomes (Powertome, U.S.A), GKM and GKM-2, glass knives (Boeckeler Instrument, U.S.A) and Fourier transform infrared microspectroscopy (FTIR-MS, Tensor 27, U.S.A) were also used.

Preparationand characterization of melatonin encapsulated niosomes

Melatonin encapsulated niosomes were prepared by a lipid thin film formation and rehydration method [10]. Molar ratio of composition of melatonin niosomes was span60:chol:SDC:melatonin 1:1:1:5. Size selection of melatonin niosomes was performed by extrusion using a polycarbonate membrane with a pore size of 100 nm (Avextin, U.S.A.). Blank niosomes were prepared by the same process but without melatonin. A previously reported method [34] was used to evaluate loading capacity and encapsulation efficiency by quantitative analysis of free melatonin in supernatant solution and the precipitated melatonin-encapsulated niosomes by UV spectrophotometry at 277 nm. The encapsulation efficiency was calculated, as the following equations:

$$\%\ \text{Encapsulation efficiency} = \frac{\text{encapsulated melatonin}}{\text{total melatonin}} \times 100$$

Triplicate samples of the melatonin niosomes were subjected to particle size analysis by using laser diffraction (Mastersizer 2000, Malvern Instruments, U.K.) and zeta potential analysis by using Zetasizer (Malvern Instruments, U.K.). Photomicrographs were taken by scanning electron microscopy (SEM, Leo 1450PV, Leo Electron Microscopy, England) by freeze-drying MN samples, mounting on stubs and then gold coating using low-vacuum sputter coating. Microscopic photographs of tissue samples were taken by an inverted microscope (Olympus IX70, Germany).

Animals

The study protocol was approved by the Institutional Committee for Ethics on Animal Experiments (AEKKU 06/2554) and was designed and conducted in accordance to the guidelines [35,36]. Male Wistar rats (total 30, average weight 150 ± 5g and aged between 4-5 weeks at starting), were obtained from, and housed at the National Laboratory Animal Center (Thailand) in a room that was acclimatized and housed at 23 ± 3°C with 55 ± 15% relative humidity and artificial lighting from 08:00 to 20:00, 150–300 Lux of luminous intensity and 10–20 air changes/h. The rats were routinely (daily) weighed and monitored for body temperature, heart rate, food consumption and behavior. Each rat was firmly held while 0.02 ml of the niosomes was gently instilled into the left nostril using a micropipette. A daily dose of 20 mg/kg melatonin BW/d for 90 days was intranasally administered to randomly assigned rats in comparison to rats assigned to receive intranasal instilled water or blank niosomes as the negative control groups (n = 4 each).

FTIR analysis

Upon completion of each study, the rats were subjected to intra-peritoneal injection of Nembutal® 60 mg/kg. Immediately after sacrifice, tissue samples of each organ were removed and frozen at -20°C. Cryosections of approximately 8-10 µm thick sections were laterally cut from each organ after fixing in OTC liquid (Tissuetek, U.S.A.). Brain sections were trimmed about 3 mm from the cerebrum coronally into the middle lobe from the position of hypothalamus of Bregma -3.00 – 3.12 mm and Interaural 6.00-5.88 mm [37]. Nasal tissue samples laterally sliced from the left nostril of each rat and nasal vestibule which contained ciliated nasal epithelium cells, non-ciliated cells and basement membrane were selected from about 10 slices. The left lobe of the liver was separated, fixed and cross-sectioned sliced for about 2 mm until reaching the middle of the tissue sample, observed as the largest area of tissue slice, and then mounted on Ag/SnO_2 or low e-slides (Kevley Technologies, U.S.A.) for FTIR-MS analysis. In each of the planes, the first and third sections (0.01 mm in thickness) were thaw- mounted of the slide surface of the low-e slides. The samples were kept in a humidity-controlled chamber.

The FTIR spectrum of each sample was scanned in reflection mode over the spectral range of 4000 – 800 cm^{-1} at spectral resolution of 4 cm^{-1} with 64 scans and an aperture size of 70 × 70 µm. The background spectra were acquired from a free area of the low-e slide and was measured every 5 spectra from the sample. FTIR spectra were processed using OPUS NT 6.5 the Unscrambler 10.1 software (Bruker Optics, GermanyCAMO, Oslo, Norway). Second derivative spectra, obtained using a Saviztky–Golay smoothing function (913 points) and vector normalized spectra using extended multiplicative signal correction to account for differences in sample thickness, were calculated to minimize baseline differences and allow easy visual comparison. Integrated areas were calculated for bands attributable to protein (amide II; 1565–1515 cm^{-1}) and lipid (ester carbonyl; 1750–1720 cm^{-1}). PLS-DA was applied to about 150 infrared spectra of each sample.

Results and Discussions

The melatonin-encapsulated niosomes (Figure 1) showed well-defined spherical vesicles with particles sizes of about 84 – 102 nm which corresponded to the average diameter of 86 ± 3 nm obtained from the laser diffraction method. An average zeta potential of -54.4±0.6 mV indicates a negatively charged interface which could prevent particle aggregation and therefore high stability. Encapsulation efficiency of melatonin in this noisome formulation was about 95 ± 0.1%, indicating that the nanosized niosomes with the use of co-surfactants, span60 and sodium deoxycholate, could associate melatonin at a proportionally high extent.

Normally, endogenous melatonin is produced by the pineal gland during the night time about 21:00 with a peak between 1-4 am [25]. After that the level of physiological melatonin reduces to a trough level at daytime; thus the time of sacrifice was about 10 am to 2 pm to minimize

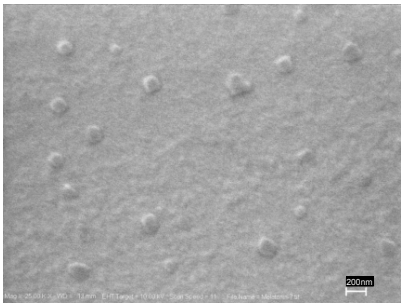

Figure 1: Scanning electron microscopic photograph of melatonin-encapsulated niosomes (25,000×)

effects of endogenous melatonin. Control groups allowed monitoring of endogenously produced melatonin, which could generally be lower than 10 pg/ml [38].

An FTIR spectrum of pure melatonin standard showed major peaks of functional groups at 3306 and 3260 cm^{-1} (N-H bending and C-N stretching), 1492 and 1550 cm^{-1} (aromatic –C=), 1630 cm^{-1} (C=O), 1180 and 1217 cm^{-1} .(-C-O)in agreement with previous studies [39,40].

After intranasal administration of repeated doses of a total of 180 mg/kg, divided into 20 mg/kg/d for 90 d, infrared mapping and imaging techniques were introduced to chemically investigate based on peak areas under specific bands of tissue components. The tissue samples selected were nasal epithelium as the first area exposed to the instilled melatonin niosomes. This route is potentially a transport path of melatonin to the brain [41], and the rats showed signs of about 15 min sedation after each dose, thus potentially affecting hypothalamus which was, thus, analyzed by FTIR. Liver is the vital organ which mainly metablized melatonin, thus subjected to the analysis.

Microscopic pictures of nasal epithelium exposed to 90 d repeated doses of 20 mg/kg/d of melatonin in niosomes was illustrated in Figure 2(b) in comparison to that of the negative control, shown in Figure 2(a) did not remarkedly detect any difference. FTIR spectra of the intervention and control group, Figure 2(c) resembles with the peaks at 1080, 1210, 1235, 1290, 1340, 1395, 1465, 1550, 1650, 2850, 2870, 2920 and 2960 cm^{-1}. The extent of the second derivatives, Figure 2(d), was slightly deviated at 1656 and 1546 cm^{-1} without shifting. PLS-DA analysis showed moderate correlation and low discrimination ($p > 0.05$). It is implied that no clear biochemical changes were detected and assumed that the melatonin niosomes at a repeated dose of 20 mg/kg/d did not affect the nasal epithelium.

Cryosections of the hypothalamus from the treatment group showed microscopic resemblance to that of the control group, as shown in Figure 3(a), 3(b). FTIR spectra of the intervention group, Figure 3(c), showed higher peaks at 1400, 1465 and 1750 cm^{-1}, the shoulder peaks at 2960 cm^{-1} for CH_3 asymmetric stretching as well as smaller peaks at 1465 cm^{-1} from CH_2 bending, mainly lipids, were slightly different. Amides I and II, at 1650 and 1550 cm^{-1}, respectively, resemble while the shoulder peaks at 1750 cm^{-1} of carbonyl stretching mainly from lipids were deviated. PLS-DA of the FTIR spectra within these regions between hypothalamus samples of treated and control groups could differentiate these deviations, which were shown to be well correlated ($r^2 = 0.97$).

Liver samples subjected to FTIR analysis gave results as shown in Figure 4, indicate dominant peaks of Amide I and II at 1650 and 1550 cm^{-1}. Rats receiving repeated doses detected some changes at wave numbers 2850 and 2920 cm^{-1}, mainly corresponding to CH_2 stretching mainly lipids, and those 2870 cm^{-1} and 2960 cm^{-1} corresponding to CH_3 symmetric stretching of lipids and proteins, similar to the previously reported FTIR spectra of normal liver tissue of rats [42]. These suggest some cumulative effects of melatonin on lipid, potentially at the cell or

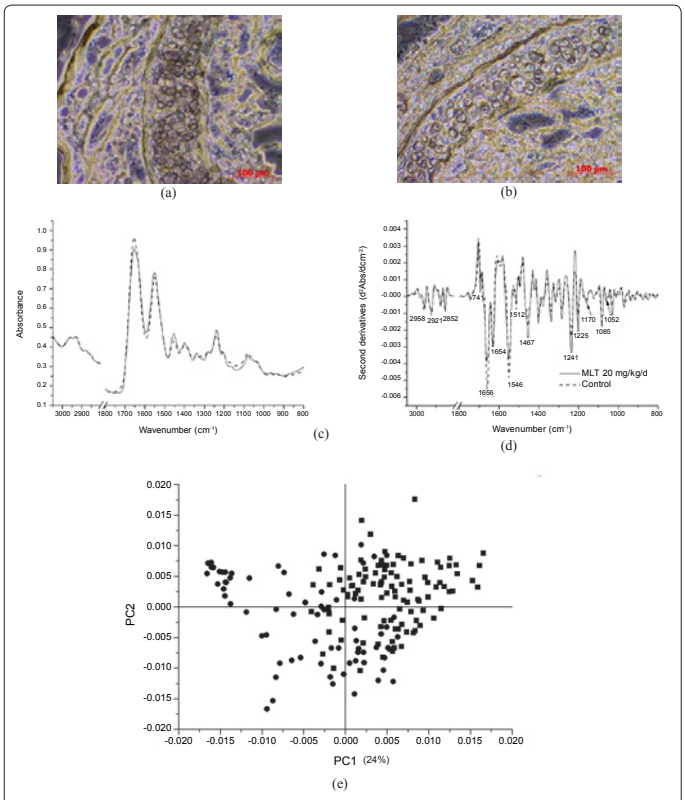

Figure 2: Analysis of microtomed section of the nasal cavity of rats: microscopic photographs (20×) of (a) the control and (b) the intervention receiving a repeated dose of MN 20 mg/kg. (c) FTIR spectra of the control (dot line) and the intervention (solid line); (d) the relevant second derivatives of the same spectra normalized by extended multiplicative signal correction; (e) PLS-DA analysis of FTIR spectra of the control (●) and intervention groups (■) and (f) prediction data from the PLS-DA analysis

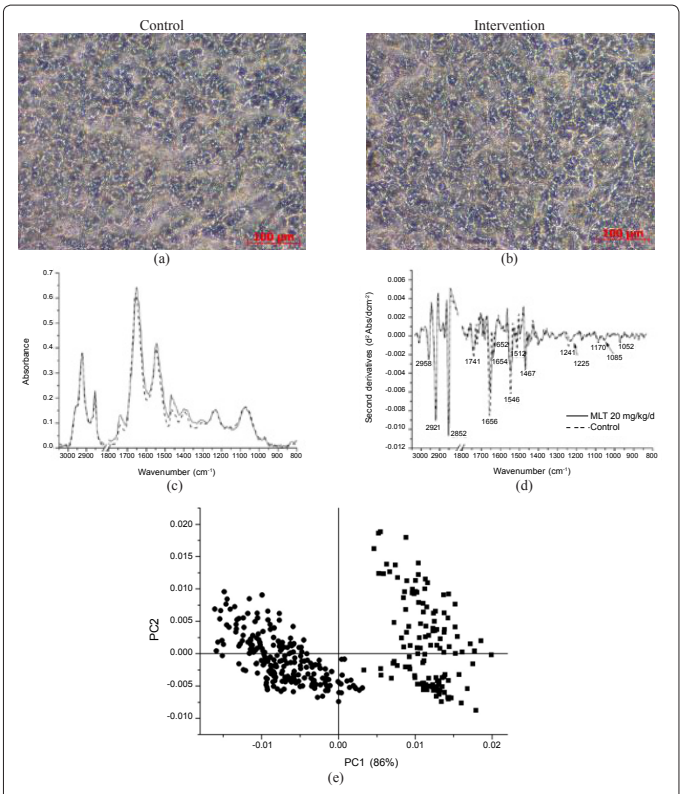

Figure 3: Analysis of microtomed section of the hypothalamus of rats: microscopic photographs (20×) of (a) the control and (b) the intervention receiving a repeated dose of MN 20 mg/kg. (c) FTIR spectra of the control (dot line) and the intervention (solid line); (d) the relevant second derivatives of the same spectra normalized by extended multiplicative signal correction; (e) PLS-DA analysis of FTIR spectra of the control (●) and intervention groups (■) and (f) prediction data from the PLS-DA analysis

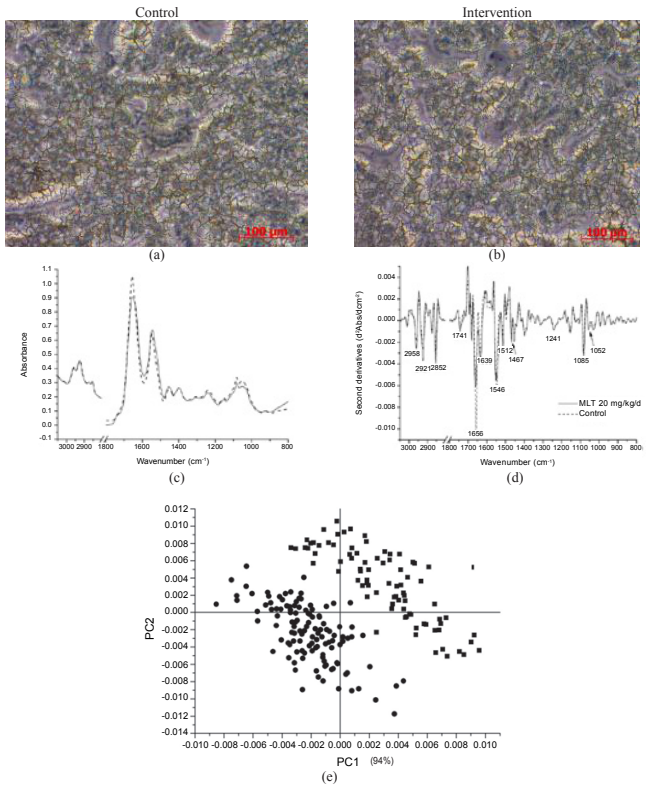

Figure 4: Analysis of microtomed section of the liver of rats: microscopic photographs (20×) of (a) the control and (b) the intervention receiving a repeated dose of MN 20 mg/kg. (c) FTIR spectra of the control (dot line) and the intervention (solid line); (d) the relevant second derivatives of the same spectra normalized by extended multiplicative signal correction; (e) PLS-DA analysis of FTIR spectra of the control (●) and intervention groups (■) and (f) prediction data from the PLS-DA analysis

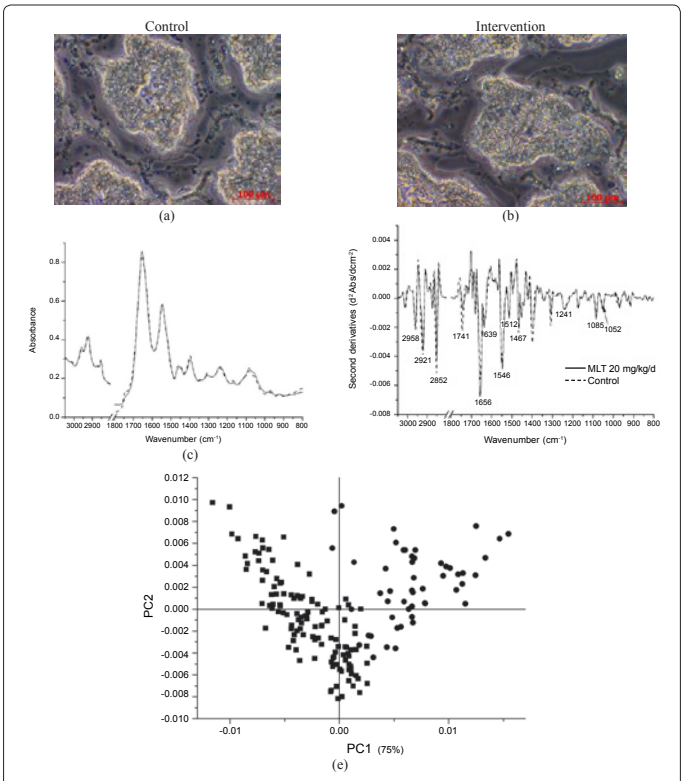

Figure 5: Analysis of microtomed section of the testis of rats: microscopic photographs (20×) of (a) the control and (b) the intervention receiving a repeated dose of MN 20 mg/kg. (c) FTIR spectra of the control (dot line) and the intervention (solid line); (d) the relevant second derivatives of the same spectra normalized by extended multiplicative signal correction; (e) PLS-DA analysis of FTIR spectra of the control (●) and intervention groups (■) and (f) prediction data from the PLS-DA analysis

nuclear membrane [32]. PLS-DA of the liver samples from the single dose group showed score plots of the 2 non-distinctive areas in the principal components, Figure 4(e), however, those from intervention group gave linear correlated score plots (r^2 = 0.94). This suggests that repeated doses of intranasal melatonin niosomes influenced some changes in the liver cells, the main site of its metabolism.

Microscopic pictures of testis samples of control and repeated dose groups showed morphological similarities between treatment and control groups, Figure 5(b), 5(a). FTIR spectra of the treated and control groups define dominant peaks at 1650 and 1550 cm^{-1}, respectively, representing Amides I and II, while the shoulder peaks at 1750 cm^{-1} of carbonyl stretching mainly from lipids were deviated. PLS-DA of the FTIR spectra within the regions between 3050-800 cm^{-1} of the testis was correlated (r^2 = 0.91).

Melatonin, a small size amphiphilic substance with high partition coefficient value, i.e. log P of 1.2 [43], is preferentially located at hydrophilic/hydrophobic interfaces and could disorder the phospholipids at CH_2 asymmetric stretching and strong hydrogen bonding with carbonyl stretching and PO^{2-} group. Melatonin has been shown to influence membrane properties by partitioning into the bilayers and locating at the bilayer-water interface [44]. It can easily cross all the anatomic barriers including blood brain barrier [40] or transport from nose to brain [41]. Exogenous melatonin could disorient the dynamic of lipids and induce a stretching in hydrogen bonding between the functional groups of melatonin in the membrane of the brain [28]. This structural arrangement enables melatonin to protect all cellular materials from oxidant agent. Tissue distribution of melatonin in this study was shown to be in line with previous reports [21,22], but shown to be affecting lipids or fatty acids, potentially the membrane of cells, mitochondria or nucleus, rather than proteins [45]. Niosomal structure with lipid and surfactants formed as vesicles may also accommodate melatonin and promote its systemic delivery into inner organs. Liposomes with small unilamellar vesicles and a diameter of 25-50 nm have been known as active targeting nanocarriers due to their smaller size but low drug load efficiency and poor stability limit their usage [47].

Since the dose of melatonin used in this study was intended to be at the borderline of that known to cause sedative side effect by intraperitoneal and intraveneous injections [46], it was not a toxic level which caused obvious histological changes in the tissues. The use of surfactants in this niosomal formulation did not cause histological damage to the nasal epithelium as shown in a previous report [48]. Melatonin distributed rapidly in vivo and care was taken to avoid the circadian effects in the study design. At the subcellular level, melatonin can interact with lipids of biological membrane [28] and preferentially forms H-bonds between N-H group of the melatonin and polar groups of surfactants [44]. Its cytoprotective effect, potentially a result of enhanced cellular respiratory function of mitochondria in which melatonin level is higher than that in plasma [15], means that it might not be possible to monitor its fate in the body by conventional methods.

Our histological observations and FTIR results gave complimentary information. Despite minute concentrations of melatonin which could interact with the complexities of the biomolecules involved in its biochemical mechanisms, the FTIR used in this study was shown to be able to detect small changes in overall tissue compositions after delivery by nanosized niosomes without tissue extraction by solvents.

Conclusions

Intranasal administration of nanosized melatonin-encapsulated niosomes at 20 mg/kg/d for 90 days was shown to distribute to the brain, liver and testis by FTIR analysis. Hence, the delivered melatonin niosomes caused some interaction with cellular lipids, and possibly expression of some cellular protein, without causing cellular damage.

Acknowledgements

The Thai Research Fund – Master Research Grants (MRG-WI535S025), the Graduate School at Khon Kaen University and General Drug House Company are thanked for the partial financial supports. Synchrotron Light Research Institution of Thailand, KKU Melatonin Research Group and Dr Somchai Pinlaor, Department of Pathology at Khon Kaen University, are thanked for contributions, support and provision.

References

1. Davis ME, Chen ZG, Shin DM (2008) Nanoparticle therapeutics: an emerging treatment modality for cancer. Nat Rev Drug Discov 7: 771-782.
2. Yiv SH, Uckun FM (2012) Lipid spheres as attractive nanoscale drug delivery platforms for cancer therapy. J Nanomedic Nanotechnol 3: 1.
3. Siddiqui IA, Shukla Y, Mukhtar H (2011) Nanoencapsulation of natural products for chemoprevention. J Nanomedic Nanotechnol 2: 6.
4. Pouton CW, Wagstaff KM, Roth DM, Moseley GW, Jans DA (2007) Targeted delivery to the nucleus. Adv Drug Delivery Rev 59: 698-717.
5. Nie S (2010) Understanding and overcoming major barriers in cancer nanomedicine. Nanomedicine 5: 523-528.
6. AgarwalR, Katare OP, Vyas SP (2001) Preparation and in vitro evaluation of liposomal/niosomal delivery systems for antipsoriatic drug dithranol. Int J Pharm 228: 43-52.
7. UchegbuIF, Florence AT (1995) Non-ionic surfactant vesicles (niosomes): physical and pharmaceutical chemistry. Adv Colloid Interface Sci 58: 1-55.
8. Hao Y, Zhao F, Li N, Yang Y, Li K (2002) Studies on a high encapsulation of colchicine by a noisome system. Int J Pharm 244: 73-80.
9. Manosroi A, Jantrawuta P, Manosroi J (2008) Anti-inflammatory activity of gel containing novel elastic niosomes entrapped with diclofenac diethyl ammonium. Int J Pharm 360: 156-163.
10. UchegbuIF, Vyas SP (1998) Non-ionic surfactant based vesicles (niosomes) in drug delivery. Int J Pharm 172: 33-70.
11. Nasr M, Mansour S, MortadaND, Elshamy AA (2008) Vesicular aceclofenac systems: a comparative study between liposomes and niosomes. J Microencapsul 25: 499-512.
12. Xu Y, Hanna M (2006) Electrospray encapsulation of water-soluble protein with polylactide. Effects of formulations on morphology, encapsulation efficiency and release profile of particles. Int J Pharm 320: 30-36.
13. Mills E, Wu P, Seely D, Guyatt G (2005) Melatonin in the treatment of cancer: a systematic review of randomized controlled trials and meta-analysis. J Pineal Res 39: 360-366.
14. Wang YM, Jin BZ, Ai F, Duan CH, Lu YZ, et al. (2012) The efficacy and safety of melatonin in concurrent chemotherapy or radiotherapy for solid tumors: a meta-analysis of randomized controlled trials. Cancer Chemother Pharmacol 69: 1213-1220.
15. Reiter RJ, Tan DX, Mayo JC, Sainz RM, Leon J, et al. (2003) Melatonin as an antioxidant: biochemical mechanisms and pathophysiological implications in humans. Acta Biochim Pol 50:1129-1146.
16. Lissoni P, Chilelli M, Villa S, Cerizza L, Tancini G (2003) Five years survival in metastatic non-small cell lung cancer patients treated with chemotherapy alone or chemotherapy and melatonin: a randomized trial. J Pineal Res 35: 12-15.
17. van den Berg MP, Merkus P, Romeijn SG, Verhoef JC, Merkus FWHM (2004) Uptake of melatonin into the cerebrospinal fluid after nasal and intravenous delivery: studies in rats and comparison with a human study. Pharm Res 21: 5.
18. Ugwoke MI, Agu RU, Verbeke N, Kinget R (2005) Nasal mucoadhesive drug delivery: Background, applications, trends and future perspectives. Adv Drug Delivery Rev 57: 1640-1665.
19. Illum L (2002) Nasal drug delivery: new developments and strategies. Drug Discovery Today 7: 1184-1189.
20. Illum L (2003) Nasal drug delivery - possibilities, problems and solutions. J Controlled Release 87: 187 -198.
21. Messner M, Hardeland R, Rodenbeck A, Huether G (1998) Tissue retention and subcellular distribution f continuously infused melatonin in rats under near physiological conditions. J Pineal Res 25: 251-259.
22. Veneas C, Garcia JA, Escames G, Ortiz F, Lopez A, et al. (2012) Extrapineal melatonin:analysis of its subcellular distribution and daily fluctuations. J Pineal Res 52: 217-227.
23. Mordechai S, Sahu RK, Hammody Z, Mark S, Kantarovich K, et al. (2004) Possible common biomarkers from FTIR microspectroscopy of cervical cancer and melanoma. J Microsc 215: 86-91.
24. Zhang Q, Jiang X, Jiang W, Lu W, Su L, et al. (2004) Preparation of nimodipine-loaded microemulsion for intranasal delivery and evaluation on the targeting efficiency to the brain. Int J Pharm 275: 85-96.
25. Brzezinski A (1997) Melatonin in human. N Engl J Med 336: 186-195.
26. Kneipp J, Beekes M, Lasch P, Naumann D (2002) Molecular changes of preclinical scrapie can be detected by infrared spectroscopy. J Neurosci 22: 2989-2997.
27. German MJ, Hammiche A, Ragavan N, Tobin MJ, Cooper LJ, et al. (2006) Infrared spectroscopy with multivariate analysis potentially facilitates the segregation of different types of prostate cell. Biophys J 90: 3783-3795.
28. Akkas SB, Incib S, Zorlu F, Severcan F (2007) Melatonin affects the order, dynamics and hydration of brain membrane lipids. J Molecular Structure 834-836: 207-215.
29. Andronie L, Panzaru SC, Cozar O, Domsa I (2011) FT-IR spectroscopy for human colon tissue diagnostic. Romanian J Biophys 21: 85-91.
30. Kamma-Lorger CS, Wehbe K, Boote C, Meek KM, Cinque G (2011) FTIR has the potential to detect stem cells in the bovine corneal stoma. J Physic Chem Biophysic 1:10000103.
31. Jackson M, Mantsch HH (1995) The use and misuse of FTIR spectroscopy in the determination of protein structure. Crit Rev Biochem Mol Biol 30: 95-120.
32. Karbownik M, Reiter RJ, Qi W, Garcia JJ, Tan DX, et al. (2000) Protective effect of melatonin against oxidation of guanine bases in DNA and decreased microsomal membrane fluidity in rat liver induced by whole body ionizing radiation. Mol Cell Biochem 211:137-144.
33. Schaing A, Varmuza K, Schreiner M (2009) Classification of synthetic organic pigments by multivariate data analysis of FTIR spectra. e-Preservation Sci 6: 75-80.
34. Xu Y, Du Y (2003) Effect of molecular structure of chitosan on protein delivery properties of chitosan nanoparticles. Int J Pharm 250: 215-226.
35. The Commission of the European Communities (2007) Commission recommendation on guidelines for accommodation and care of animals used for experimental and other scientific purposes. Brussels: Official Journal of the European Union.
36. OECD (2009) Guideline for the testing of chemicals TG 413 on subchronic inhalation toxicity - 90-day study. Paris: Organization of Economic Co-operation and Development.
37. Paxinos G (2009) Figure 58-59 in The rat brain in stereotaxic coordinates - the new coronal set. 5thEdition. San Diego: Academic Press.
38. Arendt J (1998) Melatonin and the pineal gland: influence on mammalian seasonal and circadian physiology. Rev Reprod 3: 13-22.
39. Szmuszkovicz J, Anthony WC, Heinzelman RV (1960) Synthesis of N-Acetyl-5-methoxytryptamine. J Org Chem. 25: 857-859.
40. Maharaj DS (2003) An investigation into the physiochemical and neutroprotective

properties of melatonin and 6-hydroxymelatonin. PhD (Pharmacy) Thesis:Rhodes University.

41. Jayachandra Babu R, Dayal PP, Pawar K, Singh M (2011) Nose to brain transport of melatonin from polymer gel suspension: a microdialysis study in rats. J Drug Target 19: 731-740.

42. Crupi V, Majolino D, Migliardo P, Mondello MR, Pergolizzi S, et al. (2004) FTIR spectroscopy for the detection of liver damage. Spectroscopy 18: 67-73.

43. Kikwai L, Kanikkannan N, Babu RJ, Singh M (2002) Effect of vehicle on the transdermal delivery of melatonin across porcine skin in vitro. J Control Release 83: 307-311.

44. Bongiorno D, Ceraulo L, Ferrugia M, Filizzola F, Giordano C, et al. (2004) 1H-NMR and FT-IR study of the state of melatonin confined in membrane models: location and interactions of melatonin in water free lecithin and AOT reversed micelles. ARKIVOC (v): 251-262.

45. Petrosillo G, Di Venosa N, Pistolese M, Casanova G, Tiravanti E, et al. (2006) Protective effect of melatonin against mitochondrial dysfunction associated with cardiac ischemia- reperfusion: role of cardiolipin. FASEB J 20: 269-276.

46. Sugden D (1983) Psychopharmacological effects of melatonin in mouse and rat. J Pharmacol Exp Ther 227: 587-591.

47. Chapman M, Pascu SI (2012) Nanomedicine design: approaches towards the imaging and therapy of brain tumours. J Nanomedic Nanotechnol S4: 006.

48. Zhou M, Donovan MD (1996) Recovery of the nasal mucosa following laureth-9 induced damage. Int J Pharm 130: 93-102.